Kodaikanal Obs. Bull. Ser. A (1977) 2, 75-84.

EARLY NEBULAR STAGE OF NOVA CYGNI, 1975

T. P. PRABHU

ABSTRACT

The emission line profiles of the spectrum of the envelope of Nova V1500 Cyg. 1975 are studied. The spectral region covers λλ 3700-4500, Hβ and λλ 6500-8800. The velocity structure of the profiles and the time variation of both the velocities and intensities of the emission peaks of Hα are interpreted as due to an expanding system of rings at different latitudes with respect to a common polar axis. The envelope was optically thick to Balmer line radiation and was thinning out rapidly during the period of observation.

Key Words: Nova Cygni 1975—nebular stage—spectroscopy—envelope model

1. Introduction

Nova Cygni 1975 (V1500 Cyg; $\alpha_{1950} = 21^h\ 09^m\ 53^s$, $\delta_{1950} = +47°\ 56'\ 41''$) was discovered on Aug 29, 1975 while still on the rising part of the light curve. It attained a maximum of $m_v = 1^m.8$ on Aug 30.85 (de Vaucouleurs, 1975), and declined at a rate of about 0.75 mag/day for the first three magnitudes. This rate is very much higher than that of Nova CP Pup, 1942, one of the fastest galactic novae known, whose rate of decline was only 0.4 mag/day (Payne-Gaposchkin, 1957). Figure 1 shows a free hand light curve of Nova Cygni constructed from the V magnitudes and visual estimates as published in *IAU circulars*. The light curve of Nova CP Pup is taken from Payne-Gaposchkin (1957) and shifted to match the maxima. The rate of decline of Nova Cygni compares with the novae 1 and 2 observed by Arp (1956) in M31. The steep rate of decline, together with the large magnitude range, and the absence of diffuse enhanced and Orion absorption systems makes V1500 Cyg an exceptional nova (Truran *et al.*, 1976).

We present in this paper spectroscopic observations made in the early nebular stage of the nova and discuss the variations in the emission line structure in terms of a simple geometrical model (Sec. 4).

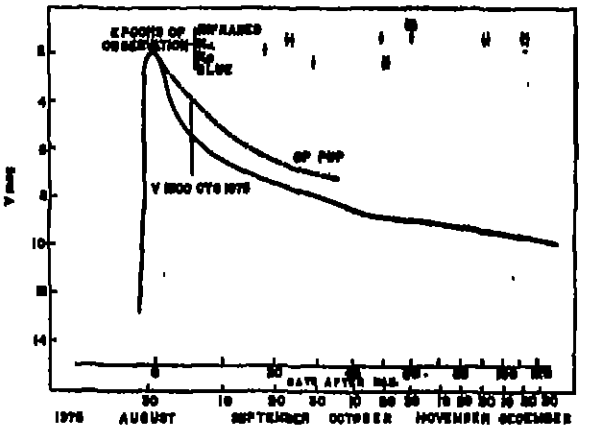

Fig. 1. Light curve of Nova V1500 Cygni (1975). The light curve of Nova CP Puppis (1942) is superposed after shifting it to match the maxima. The vertical line denotes the onset of Maclaughlin's nebular stage. The arrows indicate the dates of observations reported here.

2. Observations

Spectroscopic observations were obtained with the Cassegrain spectrograph attached to the 102-cm reflector at Kavalur. The spectrograms could be obtained only after the nova had faded to a magnitude of V $7^m.0$. By this time the spectrum of the nova had already evolved into the nebular stage. Table 1 summarises the observational data and the epochs of observation are shown as arrows in Figure 1. The calibration plates were taken with a quartz spectrograph with a continuum source and a rotating

sector. The spectra were traced on a microdensitometer.

Table 1. Observational data* on Nova Cygni 1975

Plate No.	Emulsion	Spectral Range λ†	Dispersion Å mm⁻¹	Mean Date of observation
				JD 2440000 +
3432 §	103a-D	G	23	2674.33
3438 ‖	103a-E	R	17	2677.24
3442 ‖	103a-F	R	17	2679 34
3444	103a-D	B	70	2686.10
3445 ‡§	103a-F	R	45	2701.18
3450a	103a-F	R	45	2705.05
3450b	103a-F	R	45	2705 08
3451a	103a-F	R	45	2705 09
3451b	103a-F	R	45	2705.22
3451c	103a-F	R	45	2705.25
3456 ‡§	IIa-O	B	70	2706.10
3456a	IIa-O	B	70	2707.07
3456b	IIa-O	B	70	2707.09
3459	I-N	I	410	2715.08
3460	I-N	I	410	2715 12
3461a	I-N	I	410	2716.10
3461b	I-N	I	410	2716.15
3462a	103a-F	R	45	2716.19
3462b	103a-F	R	45	2716.20
3474a	103a-F	R	45	2746.10
3477a	103a-F	R	45	2747.17
3480	103a-F	R	45	2767.12
3481	103a-F	R	45	2768.10

* All plates are widened to 400μ unless otherwise specified.
† Spectral Range : B: λλ3700-4400; G: λλ4400-5100; R: λλ 6200-6900; I: λλ6500-8800.
§ Widened to 80μ
‖ Widened to 800μ
‡ Not calibrated; mean calibrations used.

The wavelength scale was established by tracing the comparison lines beyond the extremities of the lines of interest and by linear interpolation. Though the comparison spectrum was exposed both on top and at the bottom of the nova spectrum only one of these was used for establishing the wavelength scale. The chart scales used correspond to 35 km s^{-1} mm^{-1} for Hα, 85 km s^{-1} mm^{-1} in the blue, and 130 km s^{-1} mm^{-1} in the near infrared. The tracings were measured to an accuracy of 0.5 mm on the chart.

3. Description of the Spectrum

3.1 *Observed emission lines*

The spectrum first observed by the end of September, 1975, shows the bright emission lines of hydrogen and the forbidden lines of [O III] and [Ne III] (Fig.2). The lines of [S II] and [O II] are faint (Table 2). The only other permitted line comparable to the Hydrogen lines in intensity is λ8446 of O I. This line is as bright as Hα and is more than ten times as bright as the multiplet 1 of O I at λλ 7772-75. Here we have an extreme case of O I λ8446 anomaly found in H II regions, planetary nebulae, Seyfert galaxies and quasars. It has been observed in several other novae too (e.g. Nova Herculis 1963; Andrillat, 1964). The most probable explanation is that λ8446 arises by Lyman β fluorescence in O° (Bowen, 1947) rather than by the recombination of O^+, and a large optical depth of the envelope

Table 2. Emission lines in the spectrum of Nova Cygni 1975.

Lab	Atom	Multiplet	Int	Eq. width Å	Int.	Eq Width Å
			JD 2442685.10		JD 2442706.57	
3726-29	[O II]	1 F			30 *	
3755-60	[Fe VII] + O III	2			40 *	
3835	H I	2			24	
3868	[Ne III]	1 F	10		66	171
3889	He I	2				
3889	H I	2	13		30	
3968	[Ne III]	1 F				
3970	H I	1	51		66	118
4026	He I	18			15 *	
4068-76	[S II]	1 F	11		20	83
4102	H I	1	89		89	137
4267	C II	6			30 *	
4340†	H I	1	100	72	100	106
4363	[O III]	2 F	53	38	126	132
4471	He I	14			35 *	
4861	H I	1				
			JD 2442701.18		JD 2442715.12	
6563 †	H I	1	100	2190	100	
6717-31	[S II]	2 F			11	
7065	He I	10			9	
7319-31	[O II]	2 F			10	
7593	He II	6			—§	
7751	[A III]	1 F			11	
7772-75	O I	1			9	
8446	O I	4			110	
8216	N I	2			40	
8542	Ca II	2			25	
8662	Ca II	2			20	
8680-8718	NI	1			25	

† Normalised to intensity 100.
* As on JD 2442706.10
§ Partially obscured by atmospheric O_2 band

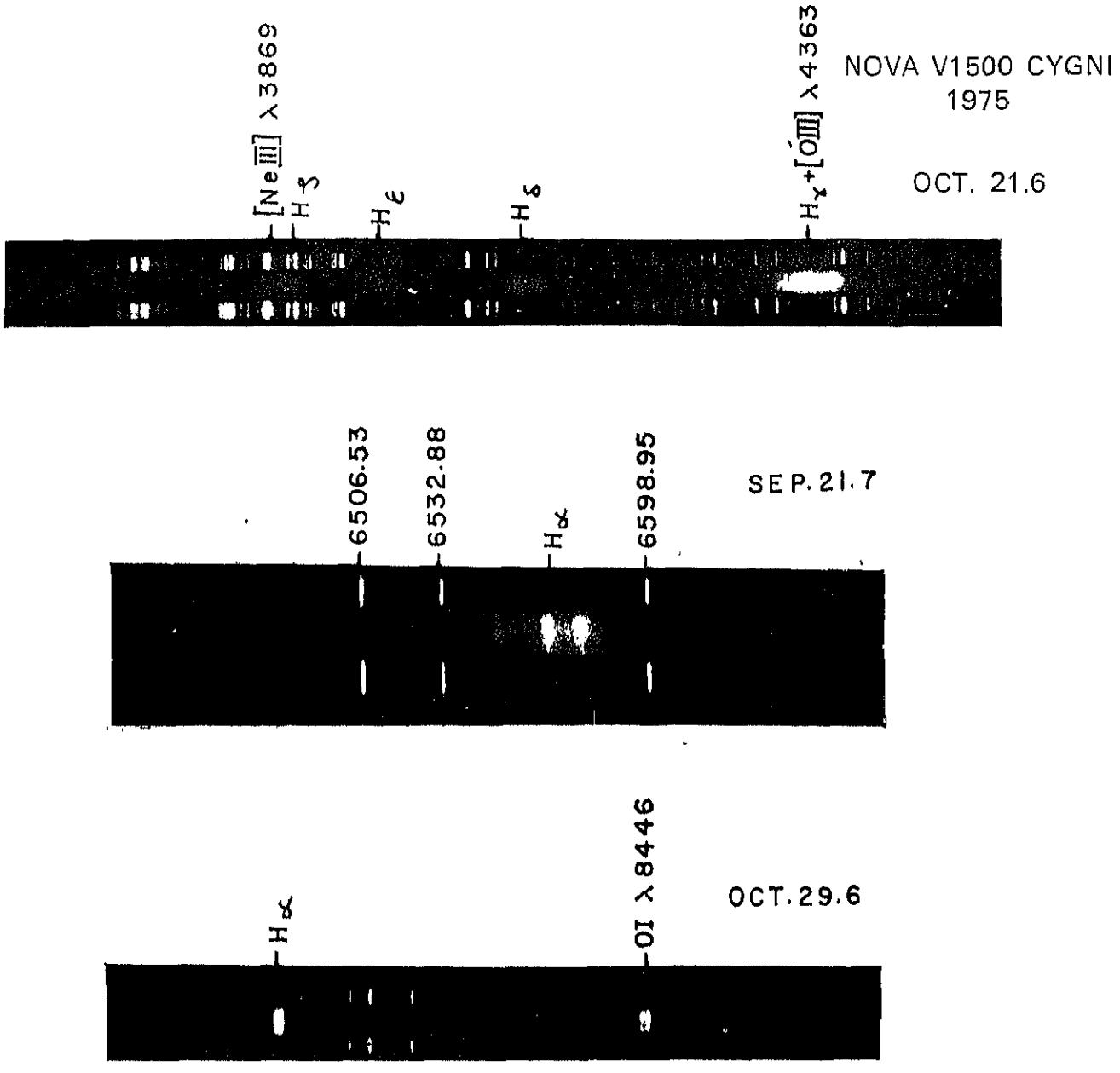

Fig. 2. Typical Spectra of Nova V1500 Cygni.

T. P. Prabhu (*facing page 76*)

increases the ratio Lyman β/Hα to the necessary value by the conversion of Hα to Lyman β. For Hα and O I λ8446 to be comparable we require optical thickness of the order of 10^3 to 10^4 in Hα (Netzer and Penston, 1976).

The forbiddden lines of [Ne III] are very strong on the plates taken in October, 1975 (β 3455, 3456a, b) while they were not seen in September (β 3444). This is an effect of decreasing electron density (N_e). Ne^+ and O^+ have similar ionization potentials (41 and 35 electron volts respectively). Hence Ne^{++} and O^{++} regions coexist. The line λ4363 is an auroral transition in O^{++} and λ3869 is a nebular line in Ne^{++}. The ratio is highly sensitive to temperature in the 10^3--10^5 K range. It is only weakly dependent on density for $N_e < 10^4$ cm^{-3}, but at higher densities the auroral transition gets stronger with respect to the nebular one. That is, I (λ3869) / I (λ4363) increases with decreasing density. We estimate that N_e was greater than 10^7 on JD 2442685 and decreased to around 10^7 to 10^6 by JD 2442706. The faintness of [O II] and [S II] lines relative to those of [O III] and [Ne III] indicates the high excitation in the envelope.

The only clearly visible permitted line other than those of Hydrogen and O I λ 8446 are He I λ 3889 (blended with H ζ), λ4026, λ4471, λ7065; C II λ4267, O I $\lambda\lambda$7772-75; Ca II λ8542, λ8662 and N I multiplets 1 and 2. The identification of N I λ8216 is doubtful since only the leading member of the multiplet 2 is seen. The feature at λ7726 could be due to C IV as suggested by Chincarini and Rosino (1964) in the case of Nova Herculis, 1963. The feature at λ3755 could be due to the multiplet 2 of O III. All these lines are very much fainter than the H I lines.

Due to the large Doppler widths of the lines, the line blending is a severe problem. The profiles of Hγ and [O III] λ4363 are severely blended, while [S II] $\lambda\lambda$4068-76 affects Hδ. Several undetected lines in the pseudo-continuum have the effect of reducing the estimates of the equivalent widths of the bright lines while the unknown contribution of the blends, when not estimated, would increase the value. The equivalent widths listed in Table 2 could be in error by a large amount.

3.2 *Profiles of bright lines*

3.2.1 *H-alpha*

Complex features in Balmer emission lines were noticeable as early as on September 3 (Leparskas, 1976). In the present investigation, Hα profiles have been observed at 22.94, 49.78, 60.85, 91.28 and 112.26 days from maximum. These Hα profiles show eleven distinct peaks which are numbered as V5, V4, V3, V2, V1, and R1, R2, R3, R4, R5, R6, (Fig.3).

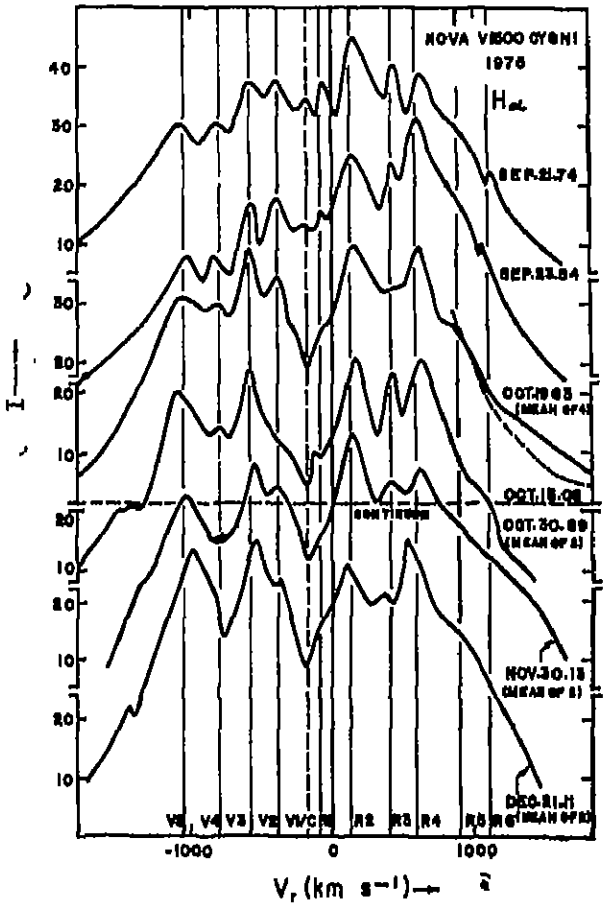

Fig. 3. The mean profiles of Hα on different epochs. The dark vertical line corresponds to zero velocity, the dashed vertical line denotes the mean velocity of the central dip, and rest of the vertical lines are the means of individual peaks. The identifications of different peaks are given in the lower portion of the figure. The continuum level is indicated for Oct. 15.

The changes in the profile are extremely systematic. As time proceeds, (i) the central dip (C) becomes more and more prominent apparently due to the gradual fading of the central peak V1 at -225km s^{-1} (ii) the violet peaks brighten in comparison with the red ones (i.e. the V peaks in Fig.3 brighten

relative to the R peaks). A comparison of the profiles of September 3 (Leparskas, 1976) and September 5 (Campbell, 1976) with our profile of September 22 (mean of JD 2442677-79) shows, however, that the changes were in the opposite direction during the early stages. The profile of September 3 shows only a red plateau fainter than the violet peaks, while by September 5, the red peaks are clearly visible and are brighter than the violet peaks. We will discuss these changes in the next section with respect to a proposed model.

The intensity changes in the various peaks during the period of observation presented in this paper are given in Table 3 referred to a constant change in the intensity of R2. This peak is chosen somewhat arbitrarily. The absolute changes or the changes relative to the continuum could not be obtained in the present investigation. The observations made on dates differing by less than three days are averaged. The average peak radial velocities reduced to Sun on different epochs are listed in Table 4. The values indicate that the radial velocities of the positive peaks are getting less positive and of the negative peaks less negative with increasing time. This effect will be discussed in sec 4.

Table 3. Changes in the intensities of the emission peaks in the H-alpha profile.

Peak	1-2	2-3	Epochs * 3-4	4-5	1-5
V5	12.16	10 72	9.12	12 74	14.96
V4	10.12	11.48	10.23	11 09	14.13
V3	10.72	10 23	9.55	12.02	12.59
V2	9.44	10.23	9.89	11.61	11.09
V1/C	9.13	9.44	10.72	10.84	8.91
†R2	10 00	10.00	10.00	10.00	10.00
R3	8.71	10.35	8.71	10.47	8.22
R4	9.12	9 66	9.12	9.66	7.33

* The epochs are 1. JD 2442678.28
2. JD 2442705.13
3. JD 2442716.20
4. JD 2442746.63
5. JD 2442767.61

† Normalised to 10

3.2.2 *Other Lines*

Apart from Hα other lines also show complex structure. The plate β 3432 obtained on JD 2442674 shows Hβ with four emission peaks (Fig.4). In spite of the problem of line blending mentioned at the beginning of this section Hγ, [O III] λ 4363, Hδ, He and [Ne III] λ 3869 show the line doubling. An attempt to separate Hγ and [O III] λ 4363 by inspection is made in Figure 6a while in Figure 6b, Hδ and [S II]$\lambda\lambda$ 4068-76 are separated. Line doubling also occurs in all the observed He I lines, in O Iλ 8446 and in [O II] $\lambda\lambda$ 7319-30 (Fig.5). The profile of [S II] 6717-31 (Fig.5) is derived from one plate where it is reduced to a rest wavelength of λ6731 and is of limited accuracy due to the faintness of the line. As in the case of Hα all the lines mentioned above also show an increase in the intensities of the violet peaks in comparison with the red ones. The average radial velocities of the components of the emission lines are given in Table 5.

Table 4. Average peak radial velocities (km s^{-1}) of Hα profile

Peak	Sep. 22.78	Oct. 18.63	Oct. 30.70	Nov 30.13	Dec. 21 1	Average
			Date (1975)			
V5	−1062	−1067	−1072	−1052	−983	−1045 ± 23
V4	−839	−786	−797	−802	–	−806 ± 14
V3	−587	−589	−597	−572	−543	−578 ± 13
V2	−402	−387	−387	−387	−335	−380 ± 15
V1	−207	(−237)	(−252)	–	(−206)	(−225 ± 14)
R1	−77	(−74)	(−72)	(−67)	(−91)	(−76 ± 5)
R2	+141	+139	+148	+133	+117	+136 ± 7
R3	+426	+426	+415	+408	+381	+407 ± 17
R4	+628	+631	+643	+620	+661	+617 ± 20
R5	–	(+900)	(+909)	(+904)	(+879)	(+898 ± 8)
R6	(+1132)	(+1133)	(+1129)	(+1128)	(+1061)	(+1117 ± 20)

Note: The values in the brackets correspond to the fainter peaks and could be comparatively less accurate.

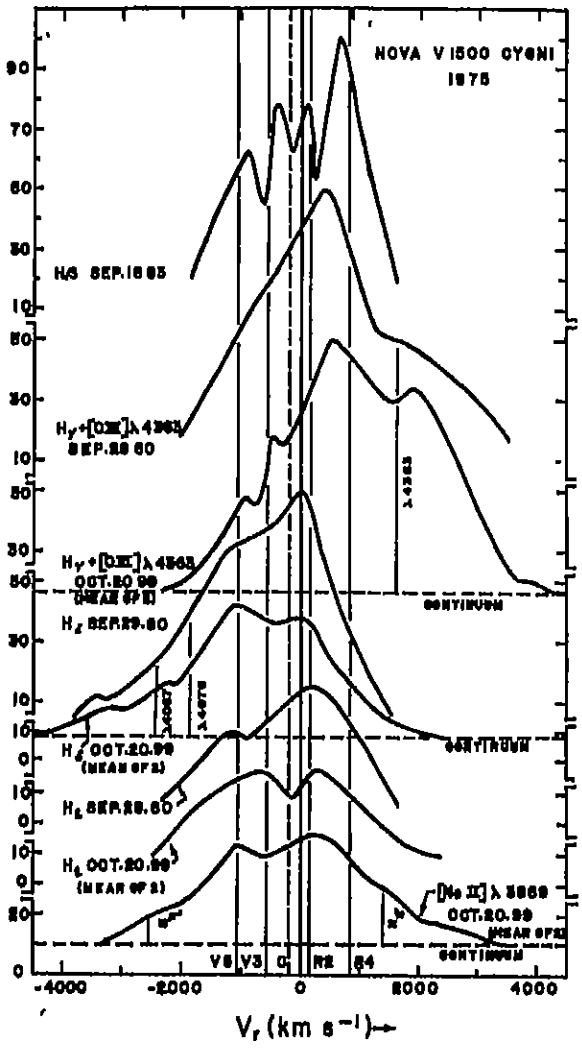

Fig. 4. The profile of Hβ and the lines in the blue region of the spectrum of Nova Cygni, 1975. Vertical lines are drawn for zero velocity, and for the central dip and prominent peaks of Hα profiles. The unshifted positions of blended lines are indicated. Continua are drawn when known. The peaks of blue lines of each epoch are normalized to a peak intensity of Hγ = 100.

4. Discussion

4.1 *Model of the envelope of V1500 Cygni*

Mustel and Boyarchuk (1970) classify nova envelopes into two kinds: (a) GK Per type, without any symmetry in their structure (b) those with a clear axial symmetry. A large number of spectroscopically and photographically studied novae fall under the second category. The photographs of the recurrent nova DQ Her (1934) have shown such symmetry from 1942 onwards, while the complex structure of the emission lines of most of the nova envelopes could be explained as a superposition of several saddle-shaped profiles of the kind obtained theoretically by Bappu and Menzel (1954) for expanding rings. Various models with rings, cones and polar caps have been computed for DQ Her (Mustel and Boyarchuk, 1970), Nova Vulpeculae 1968 (1), Nova Serpentis 1970 (Hutchings, 1972), Nova Delphini 1967 (Hutchings 1972, Malakpur 1973) and V603 Aql (Weaver, 1974).

The apparent symmetry of the peaks in the Hα and other emission line profiles of Nova Cygni indicate an axially symmetric model. An attempt is made to reconstruct the shell from the velocity structure of the emission profiles obtained in Sec. 3.

A saddle-shaped profile could result from both an expanding shell and an expanding ring. In the absence of any supporting evidence for the formation of several shells with different velocities of expansion such as multiple absorption components or auxiliary peaks in the light curve, we assume that the multiple

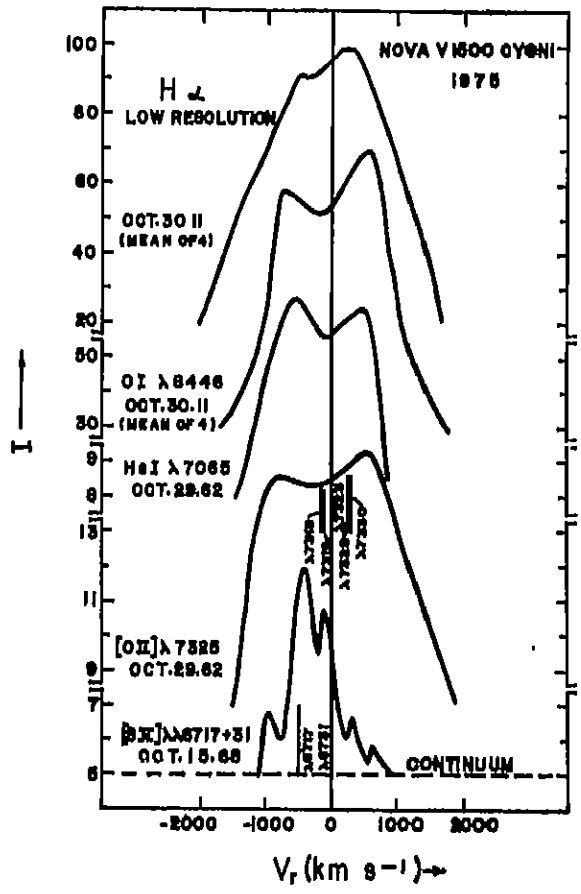

Fig. 5. The profiles of lines in the red-infrared part of the spectrum of Nova V1500 Cygni.

peaks of Hα profile of the nova arise due to a system of expanding rings situated at different latitudes about a common polar axis. If the polar axis makes an angle I (Fig.7) with the line of sight, and the ring is situated at a colatitude θ, the resultant emission profile has peaks at the velocities V_1 and V_2 given by

$$V_1 = V_0 \pm V_{exp} \cos(\theta + I) \quad (1)$$

$$V_2 = V_0 \pm V_{exp} \cos(\theta - I) \quad (2)$$

where V_0 denotes the systemic velocity of the nova and V_{exp} the expansion velocity of the ejecta. The angle θ is taken to be always acute measured from

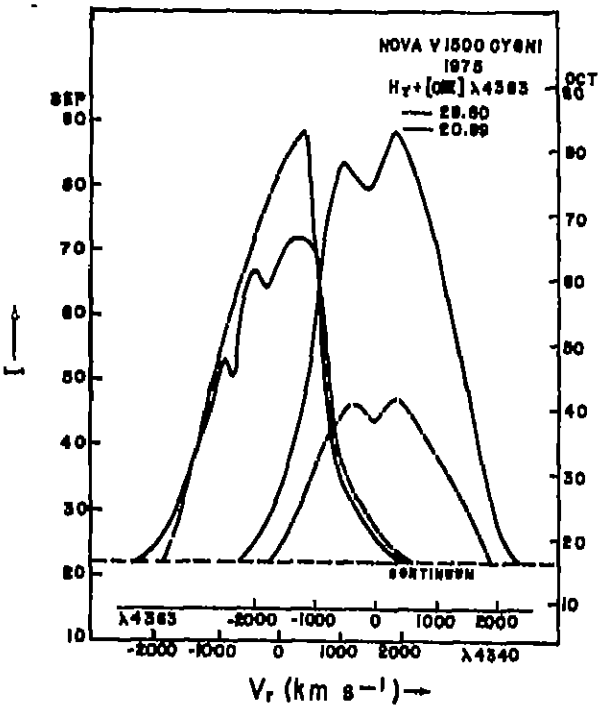

Fig. 6a. Approximate separation of Hγ and [O III] λ 4363. The continuum on Sep. 29.60 is estimated by superposing the wings of the blend over those of October profile.

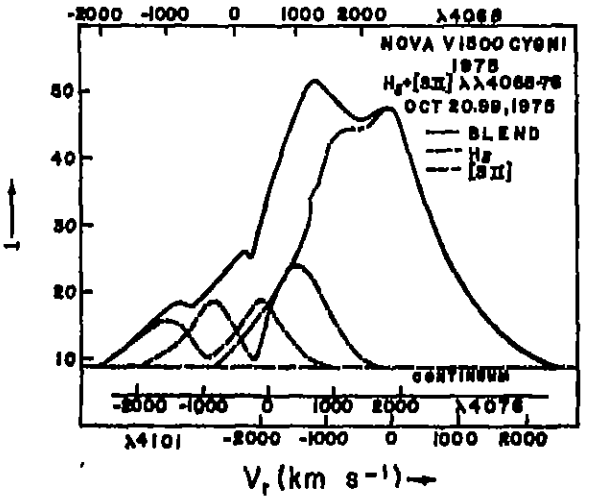

Fig. 6b. Approximate separation of Hδ, and [S II] λ 4068, λ 4076, on Oct 20.99.

other pole. The negative sign is used in the above equations when the ring is situated within 90° from the pole nearer to the observer, and the positive sign is used otherwise.

The procedure adopted in constructing the model is as follows: The systemic velocity V_o of the nova and the velocity of expansion V_{exp} of the ejecta are estimated and the proper pairs of peaks are selected as suggested by their similar behaviour with respect to the intensity variations. The angles θ and I are obtained by solving the equations (1) and (2). The agreement between the value of the inclination for different rings is taken as a check on the proper pairing of the peaks.

The effect of changing the adopted values of V_o and V_{exp} can be estimated as follows. Differentiating equations (1) and (2) we obtain

Table 5 Radial velocities (km s^{-1}) of emission peaks of various lines

Hα	Hβ	Hγ	[S II] λ6731	[S II] λ4072	Hα (low resoln)	Hδ	He	O I λ8446	[O II] λ7325	He I (mean)	[O III] λ4363	[Ne III] λ3869
− 1045 (V5)	− 910	− 980	− 950	− 850								
− 578 (V3)		− 500			− 500	− 600:	− 600:	− 700	− 850	− 600	− 500:	− 850:
− 380 (V2)	− 420		− 400									
+ 138 (R2)	+ 90	+ 100:	− 125									
+ 407 (R3)			+ 325		+ 250	+ 260	+ 260					
+ 617 (R4)	+ 700	+ 450:	+ 650	+ 500				+ 600	+ 600	+ 500	+ 375	+ 450

Note: The values marked : are uncertain due to blending.

$$dV_o \pm dV_{exp} \cos(\theta \pm i)$$
$$-V_{exp} \sin(\theta \pm i)\ (d\theta \pm di) = 0 \qquad (3)$$

Equation (3) shows that the effect of changes dV_o and dV_{exp} in the assumed values of V_o and V_{exp} respectively have an effect of changing the inferred values of θ and i by an amount of the order of dV_o/V_{exp} and dV_{exp}/V_{exp}. The contribution due to the former is very small as the errors in V_o are not comparable to the expansion velocity and the adopted value of V_{exp} cannot be in error by more than 30% (see below). The effect of this error would however be to distort the model to some extent without basically changing it. It may be added further that a latitude dependence of the expansion velocity is quite possible and this would result in a deformation of the model while its projection on a spherical surface centered on the nova would still be as obtained.

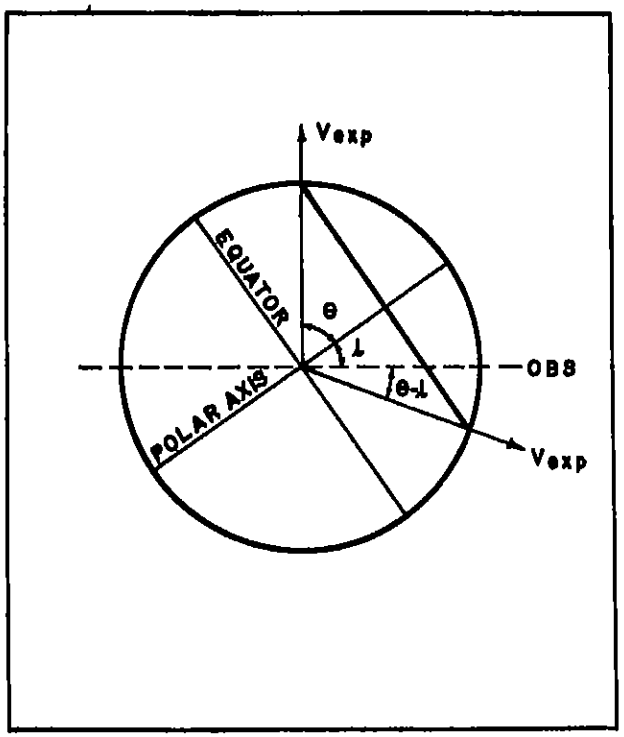

Fig. 7. The geometry of a ring situated at the latitude θ with the axis subtending an angle i with the line of sight.

Values of -1300km s^{-1} (Horn *et al.* 1975) to-2250 km s^{-1} (Woszcyk, 1975) have been measured for the absorption velocities of the nova at its early post-maximum stage. we adopt a value of V_{exp} = 1700 km s^{-1} for the following discussions. The systemic velocity of the nova could be estimated in several ways :

(a) A profile formed due to an equatorial ring or a pair of polar caps (Bappu and Menzel, 1954), or a pair of symmetrically placed rings with equal expansion velocity (Hutchings, 1972), or any combination of these has a central dip at zero velocity with respect to the central star. The central dip of the Hα profile of Nova Cygni is observed at − 180 ± 20 km s^{-1}.

(b) Sanford (1945) suggested that if "jets of matter are always shot out in diametrically opposite directions, mean values of properly selected pairs of maxima should provide a way of obtaining the radial velocity of the nova". He obtained a value of +66 km s^{-1} for Nova CP Pup which exceeded by 30 km s^{-1} the value derived from the measurements of the centres of broad emission lines.

The mean velocities of the six major peaks of Hα profile of V1500 Cygni gives value of −211 ± 6km s^{-1}.

(c) The centres of broad emission lines observed in the principal spectrum were at -75 ± 50 km s^{-1} (Bolton and Gulliver, 1975). The centre of symmetry of the profile of Hα registered on β 3445 where the continuum is also recorded changes from -100 km s^{-1} at the base of the profile to -180 km s^{-1} near the intensity maxima. The centres of symmetry of the lines other than Hα have an average value -106 ± 46 km s^{-1}.

(d) As it is believed that galactic novae belong to intermediate population I with a velocity dispersion of 60 km s^{-1} and not to a disk population, and since the position of the nova is nearly at l^{II} = 90°we cannot obtain an estimate from galactic rotation.

The high values of (a) and (b) also conflict with the supposition that novae belong to the intermediate population I, while they can be explained to be due to an asymmetry in the latitude structure of emitting rings as proposed here. We attach significance only to the values in (c) and assume an average value of -90 km s^{-1} for the systemic velocity.

The four prominent peaks in the Hα profile are V5, V3, R2 and R4. These could arise from two rings. There are three different possibilities of grouping them.

I V6-V3 ; R2-R4
II V6-R2 ; V3-R4
III V6-R4 ; V3-R2

Group III could not yield any axially symmetric model and hence only two models were constructed: one with Group I and the other with Group II. Both the models give two rings parallel to the equator corresponding to the four brightest peaks V5, V3, R2, R4. The fainter peaks V2, V4, R1, R3, R5 and R6 were paired to yield rings parallel to the first two. Table 6 lists the latitudes of each ring and the value of the inclination of the polar axis of each ring to the line of sight. The observational uncertainties in the peak velocities could amount to about ± 1° in all the angles and we note that the parallelism of different rings is ascertained within this error. The only exception is the ring due to R5-R6 in Model I which gives an inclination of about 3° less than the mean inclination. We feel that this difference is significant and adjust the value of the expansion velocity to 1350 km s^{-1} for this ring to get an agreeable inclination. This is only an alternative to an actual distortion in the envelope. Similarly the slight distortion in the rings V2-R5 and R1-R6 in Model II is an alternative to a slightly higher expansion velocity. A value of 1850 km s^{-1} used only for these two rings gives the latitudes 101°.7 and 110°.2 respectively and the inclination 20°.6 for these rings. This brings the mean inclination to the value to 20°.7 ± 0°.1. A slight distortion of the envelope or slightly differing velocities of expansion for different rings or both are quite possible (e.g. Nova Aql: Weaver, 1974). However these effects would be of secondary nature to the models proposed here. The basic models are illustrated in Figure 8.

The lines of [S II], [O II], [O III], [Ne III], O I and He I have a velocity structure slightly different from that of H I lines. The lines of [S II], [O II] and He I are faint and the inferred radial velocity structure could be uncertain. OI λ8446 is, however, as bright as Hα and shows peak velocities 200 (violet) to 350 (red) km s^{-1} higher than Hα. If as believed, the line owes its strength to the Lyman β fluorescence it should be arising just outside the H$^+$-H^0 boundary. Hence the higher separation of peaks indicates a higher expansion velocity in the outermost regions. This is further supported by the lower separations of the peaks of [O III] (I.P.=35.00) and [Ne III] (I.P.=40.91) which would be emitted predominantly from the inner regions due to their comparatively high ionization potentials. These observations indicate an increase in the expansion velocity of a few hundred km s^{-1} from the inner to to the outer regions of the envelope.

Table 6. Model parameters of the envelope of Nova Cygni 1975

$V_o \simeq -90$ km s^{-1} $V_{exp} \simeq 1700$ km s^{-1}

Model I			Model II		
Peaks	*θ (deg)	i (deg)	Peaks	*θ (deg)	i (deg)
V5-V3	64.8	8.8	V5-R2	76.7	20.8
V4-V2	72.7	7.5	V4-R3	86.1	20.9
R1-R3	98.7	8.3	V3-R4	93.9	20.7
R2-R4	106.1	8.5	V2-R5	102.9	22.7
R5-R6	130.3	4.9	R1-R6	112.3	22.9
† R5-R6	146.3	8.1			
§ Mean i	8.3 ± 0.3		Mean i	21.6 ± 0.7	

* Measured from the pole nearer to the observer
† V_{exp} reduced to 1350 Km s^{-1}
§ Excluding R5-R6

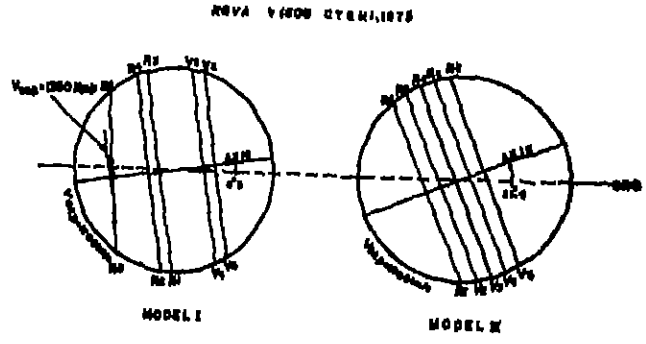

Fig. 8 Model envelopes of Nova Cygni, 1975 $V_o \simeq -90$ km s^{-1} $V_{exp} = 1700$ km s^{-1}.

Model I: $i = 8°$ and rings at roughly 65°, 73°, 89°, 106° and 130° *from the pole nearer* to the observer. The dashed line represents the last ring when its expansion velocity is *reduced to* 1350 km s^{-1} in order to make its inclination agree with the *rest* of the rings.

Model II: $i = 22°$ and rings at *roughly* 77°, 86°, 94°, 103° and 112° from the pole nearer to the observer.

4.2 Changes in the individual peaks of Hα in relation with the proposed model

The intensity changes in the peaks are indicative of the changes in the physical conditions of the envelope. The relative intensities of V5 and V3 and also V4 and V2 are changing in phase. This is especially evident in the rates of change in the intensities given in Table 7. We also see that the

rate of weakening of R4 against R2 is steady at 0.15% per day and has very small dispersion about this value. The total change in the intensities between September 22 and December 21 (epochs 1 and 5 in the table) shows a correlation with the peak velocity (Fig. 9). The latter is the line of sight component of the expansion velocity and hence the correlation reduces to a correlation between the changes in peak intensities and the angle the radius vector of the emitting region makes with the line of sight. The explanation should be based upon the emission line profiles from the optically thick rings thinning out in time, and is not attempted here.

As mentioned already (Sec. 2), in the early Hα profiles published (Leparskas 1976, Campbell, 1976) violet peaks were brighter initially and became fainter by about September 5. The recombinations could have started about this time in the outer envelope. If one uses the visual light curve to estimate the continuum flux roughly, one notices that the total emission has decreased between September 5 and October 15 indicating a substantial amount of recombinations, thus placing obscuring neutral Hydrogen atoms in front of the rings emitting the violet peaks.

We find a ϕ-dependence also in the velocity residuals defined as the deviations of the velocity on a particular date from its mean value over the total duration of observation. We list the values of $(dV_r/dt)/V_r$ in Table 8, where t is the time in days measured from the centroid of all observations. We find an average value of

$$(dV_r/dt)/V_r = (-1.6 \pm 0.5) \times 10^{-3}\,\text{day}^{-1}$$

If this is interpreted as due to the deceleration of the envelope, we obtain for a value of $V_{exp} = 1700$ km s^{-1},

$$dV_{exp}/dt = -2.7 \pm 0.8 \text{ km s}^{-1}\,\text{day}^{-1}$$

$$= -3.2 \pm 1.0 \text{ cm sec}^{-2}$$

Table 7. Rate of change of intensities of Hα emission peaks§

Peak	Epochs* 1-2	2-3	3-4	4-5	1-5
V5	+ 3.17	+ 2.71	− 1.31	+ 5.03	+ 1.96
V4	+ 0.19	+ 5.42	+ 0.33	+ 2.16	+ 1.88
V3	+ 1.12	+ 0.80	− 0.66	+ 3.83	+ 1.12
V2	− 0.93	+ 0.90	− 0.16	+ 3.11	+ 0.60
R2	0	0	0	0	0
R3	− 2.23	+ 1.35	− 1.97	+ 0.96	− 0.96
R4	− 1.49	− 1.35	− 1.31	− 1.92	− 1.51

§ The values of $(dI/I)/dT$ in the units of 10^{-3} d^{-1}.
* The epochs 1 to 5 are as described in Table 5.

Though the envelope of a nova becomes optically thin to continuum radiation at about the time of maximum light, it may continue to be optically thick to the line radiation for quite some time since the line absorption coefficient is very much larger than the continuum absorption coefficient (Pottasch, 1959). We witness an evidence to the moderate optical thickness of the envelope through the Balmer decrement (Table 2). The decrement is less steeper than the decrement in the optically thin case; the theoretical ratios of Hγ : Hδ : Hε for $T_e = 10^{4}$°K,

Table 8. The values of $(dV_r/dt)/V_r$ †

Peaks	*Epoch (Days after max). 1 22.94	2 49.76	3 60.85	4 91.28	5 112.15	Average 67.4
V5	− 0.151	− 1.197	− 3.939	+ 0.281	− 1.325	− 1.27 ± 1.05
V3	− 0.351	− 1.078	− 5.023	− 0.435	− 1.352	− 1.90 ± 2.30
V2	− 1.302	− 1.044	− 2.809	+ 0.771	− 2.646	− 1.41 ± 0.92
R2	− 0.828	− 1.254	− 13.466	− 0.926	− 3.122	− 3.92 ± 3.66
R3	− 0.994	− 2.850	− 3.008	+ 0.105	− 2.525	− 1.81 ± 0.79
R4	− 0.400	− 1.288	− 8.427	+ 0.205	− 2.020	− 1.99 ± 4.15

Weighted average − 1.57 ± 0.50

† In the units of 10^{-3} d^{-1}.
* As defined in Table 5.

$N_e = 10^4\,cm^{-3}$ are 100:55:34 (Brocklehurst, 1971) against the observed 100:89:51. These values are rough due to the difficulties of line blending and errors in the continuum level on our plates exposed for line profiles, but are yet indicative of the high optical thickness (Netzer and Penston, 1976). Furthermore the apparent decrease in the peak velocities can be explained as a result of the optical thickness decreasing with time and the radial increase of V_{exp}; as the density in the envelope decreases it exposes the inner lower velocity regions. The rate of 2.7, km s^{-1} d^{-1} which is obtained for dV_{exp}/dt gives a total change of about 250 km s^{-1} over the period of observation. This is of the same order as the maximum difference in the blue and red peak velocities of the lines due to differentions.

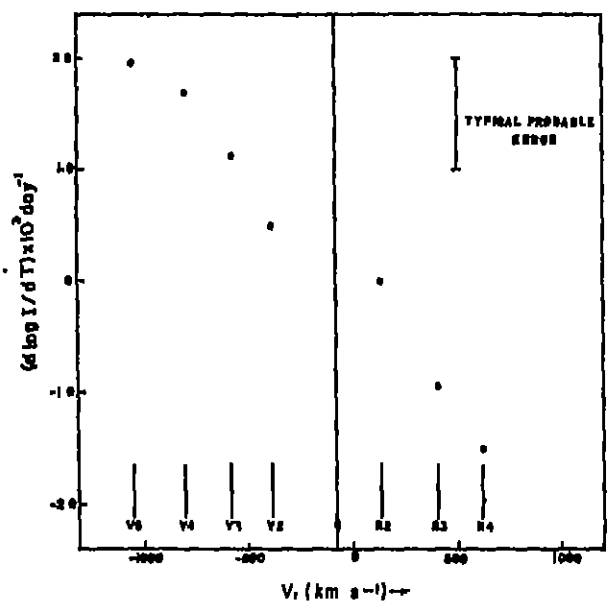

Fig. 9. The time rate of change of relative intensities of peaks in the Hα profile against the peak radial velocities. The identification of the angle $\phi = \theta \pm \beta$ are also marked. The points are derived from the total change between JD 2442678 and JD 2442768 while the typical probable error is obtained from the scatter in the rates derived from the successive epochs of observation.

5. Conclusions

Like most of the novae the observations of Nova V1500 Cyg could be explained with a model consisting of an envelope of axisymmetric rings situated at different latitudes with respect to a common axis.

This idea is supported by the velocity structure of the emission line profiles and also by the time variations of the intensities and velocities of the emission peaks of Hα line. Two geometrical models are constructed which are equally plausible (Fig. 8, Table 6).

There seems to be a linear increase in the velocity of expansion of each ring along its thickness. An estimated value for the velocity difference between the outer and the inner regions of a ring is 200 km s^{-1}.

The envelope was optically thick in Hα and possibly in other Balmer lines during the period of observations, but was thinning out rapidly.

Acknowledgments

I am very much thankful to Dr. M. K. V. Bappu for his continuous encouragement and helpful discussions. I am thankful to Dr. R. Rajamohan for his help in obtaining some of the spectra. I am grateful to Dr. D. C. V. Mallik and to Dr. N. Kameshwar Rao for reading the manuscript in detail and making numerous helpful suggestions.

References

Andrillat, Y., 1964, *Ann. Astrophys.*, 27, 475.
Arp, H. C., 1956, *Astr. J.*, 61, 15.
Bappu, M. K. V., Menzel, D. H., 1954, *Astrophys. J.*, 119, 508.
Bolton, T., Gulliver, A., 1975, *I. A. U. Circular* No: 2829.
Bowen, I. S., 1947, *Publ. astr. Soc. Pacific*, 59, 196.
Brocklehurst, M., 1971, *Mon. Not. R. astr. Soc.*, 153, 471.
Campbell, B., 1976, *Astrophys. J. Letters*, 207, L41.
Chincarini, G., Rosino, L., 1964, *Ann. Astrophys.*, 27, 469.
Horn, J., Zdarsky, F., Kriz, S., 1975, *I. A. U. Circular* No: 2827.
Hutchings, J. B., 1972, *Mon. Not. R. astr. Soc.*, 158, 177.
Leparskas, H. J. A., 1976, *Publ. astr. Soc. Pacific*, 88, 154.
Malakpur, I., 1973, *Astron. Astrophys.*, 24, 125.
Mustel, E. R., Boyarchuk, A.A., 1970, *Astrophys. Sp. Sci.*, 8, 183.
Netzer, H., Penston, M.V., 1976, *Mon. Not. R. astr. Soc.*, 174, 319.
Payne-Gaposchkin, C., 1957, *The Galactic Novae*, North-Holland Publishing Company, Amsterdam.
Pottasch, S. R., 1959, *Ann. Astrophys.*, 22, 394.
Sanford, R. F., 1945, *Astrophys. J.*, 102, 357.
Truran, J. W., Gallagher, J. S., Sparks, W. M., Strittmatter, P., Van Horn, V., 1975, *Bull. Am. astr. Soc.*, 7, 509.
Vaucouleurs, G. de, 1975, *I. A. U. Circular* No: 2839.
Weaver, H., 1974, *Highlights of Astronomy*, 3, 509.
Woszczyk, A., 1975, *I.A.U. Circular* No: 2832.